Radiation Physics and Chemistry 164 (2019) 108353

Contents lists available at ScienceDirect

Radiation Physics and Chemistry

journal homepage: www.elsevier.com/locate/radphyschem

Luminescent properties of MgB_4O_7:Ce,Li to be applied in radiation dosimetry

Luiza F. Souza[a,*], Andrea L.F. Novais[b], Patrícia L. Antonio[c], Linda V.E. Caldas[c], Dívanizia N. Souza[a]

[a] Departamento de Física, Universidade Federal de Sergipe, UFS, Av. Marechal Rondon, s/n, 49100-000, São Cristovão, SE, Brazil
[b] Faculdade de Engenharia Mecânica/Instituto de Geociências e Engenharias, Universidade Federal do Sul e Sudeste, UNIFESSPA, Folha 17, Quadra 4, Lote Especial - Nova Marabá, 68505-080, Marabá, PA, Brazil
[c] Instituto de Pesquisas Energéticas e Nucleares, Comissão Nacional de Energia Nuclear, IPEN/CNEN-SP, Av. Prof. Lineu Prestes, 2242, 05508-000, São Paulo, SP, Brazil

ARTICLE INFO

Keywords:
OSL dosimetry
Photoluminescence emissions
Magnesium tetraborate

ABSTRACT

MgB_4O_7 is a promising matrix host for use in radiation dosimetry due to its low effective atomic number (Z_{eff} = 8.2). The present work aims to investigate dosimetric and luminescent properties of the MgB_4O_7:$Ce_{0,5\%}$,$Li_{0.5\%}$, produced through solid-state synthesis, using the optically stimulated luminescence (OSL) technique. The first part of this work discusses the luminescent aspects of this phosphor, such as thermoluminescent emission spectra, photoluminescence emission, lifetime of emission centers and the effect of different lithium concentrations as co-dopant. In the second part, the basic OSL properties were evaluated, including dose-response curve, minimum detectable dose (MDD), step annealing, and best bleaching set-up for reuse of MgB_4O_7:$Ce_{0,5\%}Li_{0.5\%}$ composites. The photoluminescence and thermoluminescence emission spectra of the composites present an emission peak at UV-VIS range centered around 370 nm, which is the most suitable for OSL dosimetry; this emission is related to Ce^{3+} electronic transitions and has a luminescence center lifetime of 0.003 ms. From the step-annealing analyses, it can be seen that the OSL emission is related to different depth trap centers in the band gap. The OSL dose-response curve is linear from 0.1 Gy to 100 Gy, with a MDD around 1 mGy. These properties make this material a strong candidate for different applications in radiation dosimetry field.

1. Introduction

The optically stimulated luminescence (OSL) technique has been widely used in several procedures, including for archeological and geological dating of materials, and nowadays it is already well established in medical dosimetry. OSL dosimeters (OSLD) have been commercially available for almost two decades (Akselrod et al., 2007; McKeever, 2001; Yukihara and McKeever, 2011; Yukihara et al., 2013). The main challenge for the OSL technique has been the lack of materials for medical applications; Al_2O_3:C (aluminum oxide) and BeO (beryllium oxide) remain the only commercially available as OSL dosimeters (Sommer et al., 2008; Jahn et al., 2010). However, these materials present some limitation. For example, Al_2O_3:C is not sensitive to all kinds of radiations (e.g. neutrons), has high effective atomic number (Z_{eff} = 11.3), and although recently it has been applied in 2D dose mapping, the long luminescence lifetime of their emission centers makes the final 2D images very blurry, requiring several image corrections (Ahmed et al., 2014, 2016a, 2016b). BeO is a tissue equivalent (Z_{eff} = 7.2) dosimeter, but its high toxicity has been limiting its application. This lack of suitable OSL materials for dosimetry in the medical field encourages the research groups to investigate new luminescent phosphorus for OSL technique (Ahmed et al., 2016a, 2016b; Souza et al., 2015, 2017).

Doped MgB_4O_7 (magnesium tetraborate) is a composite extensively used in thermoluminescent (TL) dosimetry and has been a focus of interest since the early 1980s, when the first reports on its functionality for dosimetry were published (Prokic, 1986, 1993, 2007), showing a high sensitivity to ionizing radiation and for being an insulator with a wide band gap of approximately 9.5 eV (Oliveira et al., 2016a). The doped MgB_4O_7 matrix is also attractive due to its low effective atomic number (Z_{eff} = 8.2), which implies a small photon energy dependence (Yukihara et al., 2014). The tissue equivalency is important for dosimetry to avoid the application of correction factors for dose calculation. Recently the MgB_4O_7:Nd was suggested to be useful for temperature

* Corresponding author.
E-mail address: luizaf25@hotmail.com (L.F. Souza).

https://doi.org/10.1016/j.radphyschem.2019.108353
Received 16 March 2019; Received in revised form 9 May 2019; Accepted 2 June 2019

sensing applications as well (Souza et al., 2015).

Although the literature describes the MgB_4O_7 as a highly sensitive thermoluminescent dosimeter (TLD) when doped with different lanthanides, especially dysprosium and thulium, still there is a lack of information about borate application in OSL dosimetry (Yukihara et al., 2014; Prokic, 1980, 2000; Prokic and Botter, 1993; Rao et al., 2009). For such application it is required that the phosphors present some particularities, such as a light sensitive trapped charge population and a luminescence emission at ultraviolet (UV) spectral range for a better discrimination between stimulation light (generally blue or green) and OSL signal. Among all different rare earth elements, cerium is the most promising dopant, because Ce^{3+} is known to have a short luminescence lifetime (10^{-7} - 10^{-8}s) and an emission band at UV-Vis range (Dorenbos, 2000; Oliveira et al., 2016b; Yukihara et al., 2017). Moreover, the use of lithium as a co-dopant effectively increases the OSL sensitivity of MgB_4O_7:Ce, acting as a charge compensator in the substitution of divalent ions (e.g. Mg^{2+}) by trivalent lanthanide (Ce^{3+}).

Therefore, the objective of this work was to investigate important aspects related to the luminescence of MgB_4O_7:Ce,Li for its application in OSL dosimetry, such as dose-response curve, minimum detectable dose (MDD), the effect of Li concentration as co-dopant in the OSL sensitivity of MgB_4O_7:Ce, and the best optical bleaching for reuse of the samples. Moreover, the step-annealing test was performed in order to investigate the stability of the OSL trapping centers. The photoluminescence (PL) and thermoluminescence emission spectra of the samples and their luminescence lifetimes were also obtained.

2. Methodology

2.1. Material synthesis

The MgB_4O_7:Ce,Li was produced by solid-state synthesis. This route has been described in detail in previous publications (Souza et al., 2014, 2015, 2017; Subanakov et al., 2014; Azorin, 2014). For the production of material, analytical grade materials of MgO (Merck, 99.9% purity), H_3BO_3 (Merck, 99.9% purity), cerium carbonate ($Ce_2(CO_3)_3$ xH_2O- Sigma-Aldrich, 99.9% purity) and lithium carbonate ($LiCO_3$- Sigma-Aldrich, 99.9% purity) were used.

The X-ray diffraction (XRD) analyses were performed to ensure that the proper crystalline phase of MgB_4O_7 was achieved. XRD analyses were carried out using a Rigaku system, model DMAX2000. The CuK_α radiation was used with the tube operating at 40 kV/20 mA in step scan mode with steps of 2θ (°) = 0.5 in the 2θ scan interval from 10° to 80°. Samples with grain sizes less than 75 μm were used and the crystalline phases were identified through the diffraction patterns available in the PDF2 (Power Diffraction File) crystallographic database in *X'Pert High Score* Plus software. The concentration of Ce^{3+} was fixed in 0.5% weight (wt %), regarding the total mass of MgB_4O_7, which is the optimal concentration for luminescence emission of MgB_4O_7 matrix host produced by solid-state synthesis (Souza et al., 2017). The concentration of Li (Li_2CO_3) was varied from 0.1% to 2% of the total weight, in order to investigate the co-dopant concentration which improves the luminescence efficiency of the samples. Most part of analyses was performed using samples in pellet format produced by cold compaction of the powder in a hydraulic press, with 50 kgf/cm^2. Each pellet had final mass of 10.0 mg, 3.0 mm of diameter, and 2.0 mm of thickness.

2.2. Luminescent measurements and irradiations

All OSL measures were carried out in a Risø TL/OSL-DA-200 system equipped with blue light emitting diodes (emission centered at 470 nm), and Hoya U-340 filters (7.5 mm thickness, transmission between 290 and 390 nm, Hoya Corp. Tokyo, Japan) were placed in front of the photomultiplier to block the stimulation light. The irradiations were performed with a $^{90}Sr/^{90}Y$ beta-ray source, coupled to the Risø system, delivering 0.1 Gy/min (02/2017) to the sample position. All the measurements were performed in continuous wave (CW), with stimulation of 60 s. All the data analyses were based on the total area under the OSL decay curve.

For the step-annealing analyses, initially the pellets were divided into batches, with 5 pellets each one, and they were irradiated with 0.5 Gy. Next, the pellets were preheated between 50 °C and 350 °C, in steps of 50 °C, using a controlled heating rate of 10 °C/min to the desired temperature, and cooled down to room temperature. Afterwards, the OSL measures of the pellets were carried out. The MDD of MgB_4O_7:Ce,Li pellets was defined as three times the standard deviation of the background readings (3σ BG) divided by the sensitivity of the sample (dose-response curve). The background was estimated by five measurements of an un-irradiated pellet.

To obtain the TL emission spectrum of MgB_4O_7:Ce,Li, the photomultiplier was removed from the Risø system and an optical fiber, connected to an Ocean Optics HR2000 spectrometer (transmission between 200 nm and 1000 nm), was attached to the reader and upon submitting the samples to controlled heating until 450 °C, with heating rate of 1 °C/s, the wavelength emission was collected using the Spectra Suite software (Ocean Optics).

The photoluminescence (PL) and lifetime measures were performed in a spectrofluorimeter (NanoLog UV–VIS–NIR-Horiba) with a R928P photomultiplier tube equipped as the detector, Xenon lamp (CW 450 W) as the excitation source, and a bandpass filter (KV399). The luminescence decays were obtained using the same spectrofluorimeter and detector and a pulsed lamp (Xenon flash tube). All measurements were carried out at room temperature and with the same instrumental parameters. The average lifetime decay was calculated using Equation (1) (Poma et al., 2017).

$$\tau_{av} = \frac{\sum A_i \tau_i^2}{\sum A_i \tau_i} \quad (1)$$

where A_i and τ_i are the emissions and their respectively lifetime values obtained experimentally.

3. Results and discussion

3.1. XRD analyses

Initially, to guarantee that the crystalline phase of MgB_4O_7 was successfully obtained through the solid-state synthesis route, the XRD of the material was performed. The experimental XRD diffractogram of MgB_4O_7 shows good agreement with the ICSD 01-076-0666 standard crystallographic database, corresponding to magnesium tetraborate with an orthorhombic crystal system (Fig. 1).

3.2. Effect of co-dopant concentration

The effect of co-doping MgB_4O_7:$Ce_{0,5\%}$ varying the Li concentration is shown in Fig. 2. An optimum OSL signal was achieved by addiction of 0.5% of Li; above this value the OSL signal decreases, creating a quenching effect in the luminescence signal. Other works showed that an optimum OSL signal of MgB_4O_7 was achieved with 0.3% Ce doping and Li concentrations up to 10% (Yukihara et al., 2017). The optimal Li concentrations obtained in this study were much lower, showing that the solid-state synthesis is a more efficient route in incorporating the co-dopant in the crystal lattice compared to the combustion synthesis described at (Yukihara et al., 2017), which has a high degree of matter decomposition and so more losses in the starting materials. Other oxides, such as MgO:Ce, also show an increase in the luminescence when Li is added in their matrix (Yukihara et al., 2013; Oliveira et al., 2016b). All other analyses discussed in this work were performed with MgB_4O_7:$Ce_{0,5\%}$, $Li_{0.5\%}$. So, for simplicity, the matrix will be called here as MgB_4O_7:Ce,Li.

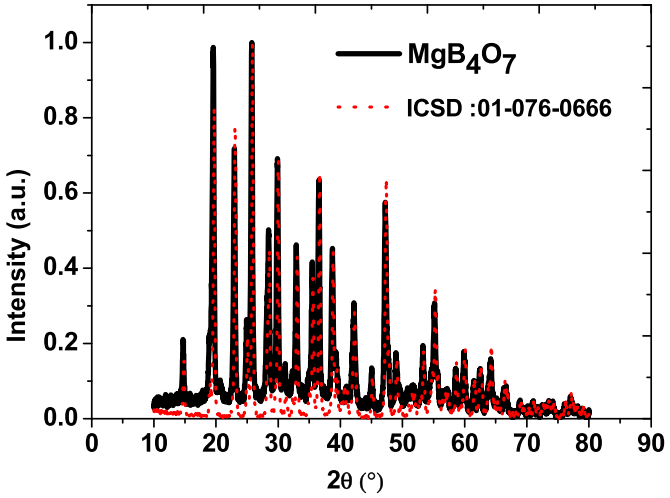

Fig. 1. Experimental XRD of MgB_4O_7 produced through solid-state synthesis and the respective reference pattern from the database ICSD 01-076-0666.

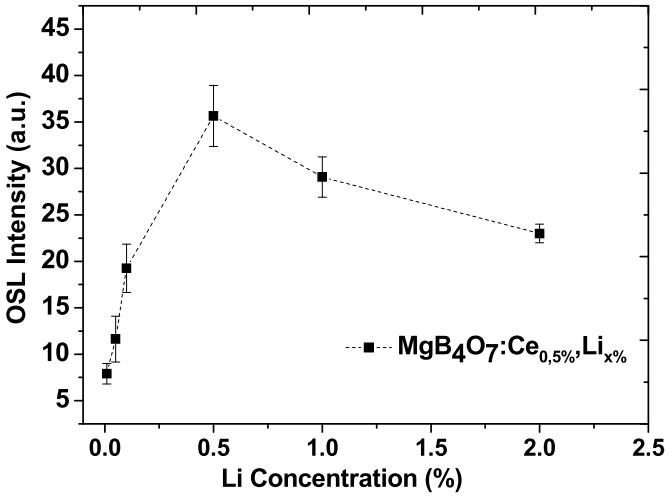

Fig. 2. OSL signal of $MgB_4O_7:Ce_{0,5\%}$ as a function of Li concentration as co-dopant.

3.3. Basic luminescent properties

In Fig. 3 is shown the TL emission spectrum of MgB_4O_7:Ce,Li, with a luminescence emission band between 350 nm and 400 nm, with a peak around 370 nm; a weaker peak is observed between 550 nm and 600 nm. These emissions are assigned to the 5d → 4f transitions from Ce^+, which are characterized by a double band due to the splitting of $^4F_1$ ground state into $^2F_{5/2}$ and $^2F_{7/2}$ states (Souza et al., 2017; Doull et al., 2014; Orante-Barron et al., 2011; Bos et al., 2011; Twardak et al., 2014).

The wavelength position of the emission band of Ce^{3+} ions is strongly affected by the crystalline field of the surrounding anions, and thus the emission of Ce^{3+} can be placed in a different position ranging in the ultraviolet-infrared (UV-IR) region, depending on the host lattice (Dorenbos, 2000; Orante-Barron et al., 2011). For MgO:Ce,Li, the main TL peak is centered at 525 nm; for other systems, such as CaO:Ce, CaS:Ce and MgS:Ce, the emissions are very similar to that of MgO, being centered at 556 nm, 505 nm and 525 nm, respectively, which are also related with the Ce^{3+} transitions (Yukihara et al., 2013; Dorenbos, 2000; Orante-Barron et al., 2011).

The PL emission of the samples, under excitation of 315 nm, shows one broad band ranging at 350–450 nm and no emission for the non-doped samples (MgB_4O_7) [Fig. 4(a)]. Additionally, the curve exhibits a shoulder ranging between 420 and 450 nm, assigned to the intrinsic luminescence of the host. The lifetime decay of the main emission was calculated through Equation (1) and is in order of 0.003 ms (3 μs) [Fig. 4 (b)].

This lifetime decay observed for the borate is higher compared to the decay of Ce at other host matrices such as CaS:Ce (bulk phosphor) presenting a lifetime decay of 1.5 μs and the CaF:Ce, CaB_4O_7:Ce and $Li_2B_4O_7$:Ce, which have lifetimes in nanosecond order (Kindrat et al., 2016; Kumar et al., 2010). However, the CaS:Ce nanophosphors have lifetime up to ms, which is attributed to more radiative relaxation caused by surface defects that act as luminescent centers (Kumar et al., 2010).

The increase in lifetime in the tetraborate may be attributed to radiative relaxation caused by the shallow traps that act as luminescent centers, increasing the radiative rate; the lifetime turns to be longer, suggesting a slower relaxation process. It is important to remind that the dynamics of emission and lifetime decays at the phosphors are governed by the interaction of the host band energy states and the dopant states, so the decay parameters also depend on the basic composition of the phosphor.

The short lifetime observed in the MgB_4O_7:Ce,Li host is extremely useful for its application in 2D dose mapping and image scanning. The

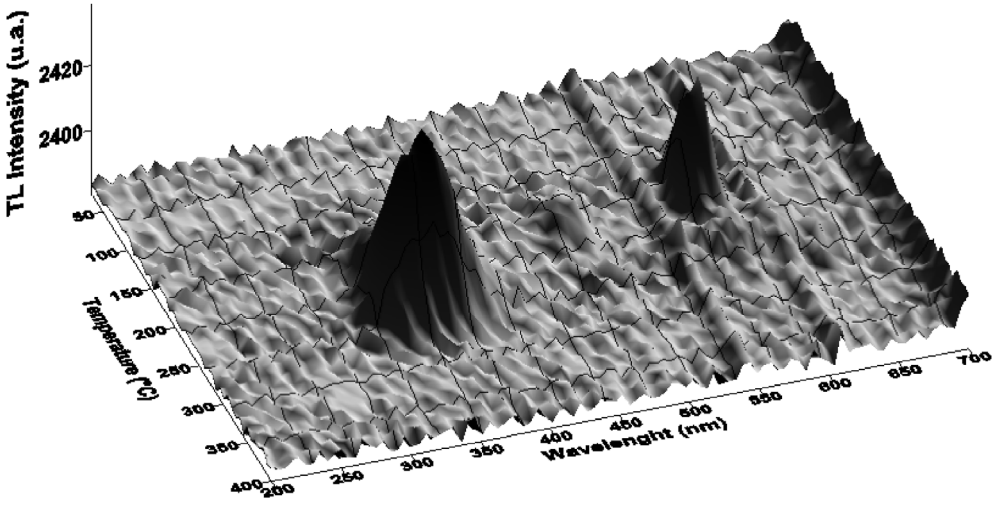

Fig. 3. TL emission spectra of MgB_4O_7:Ce,Li.

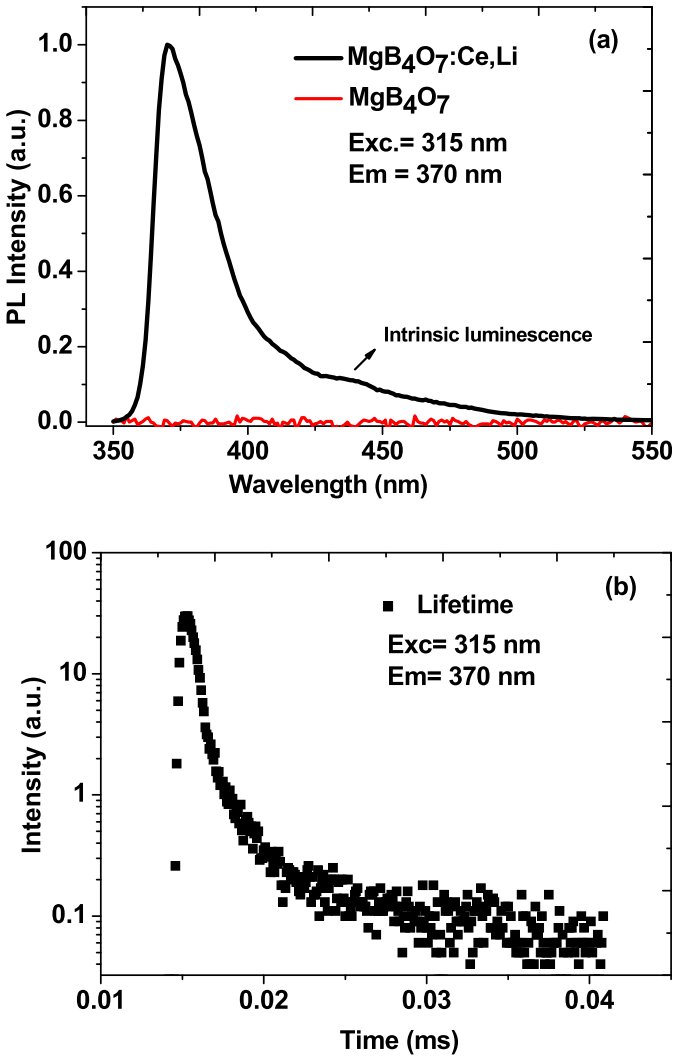

Fig. 4. (a) Emission spectra and luminescence lifetime (b) decay curves of MgB_4O_7:Ce,Li measured at room temperature, under an excitation of 315 nm laser pulse.

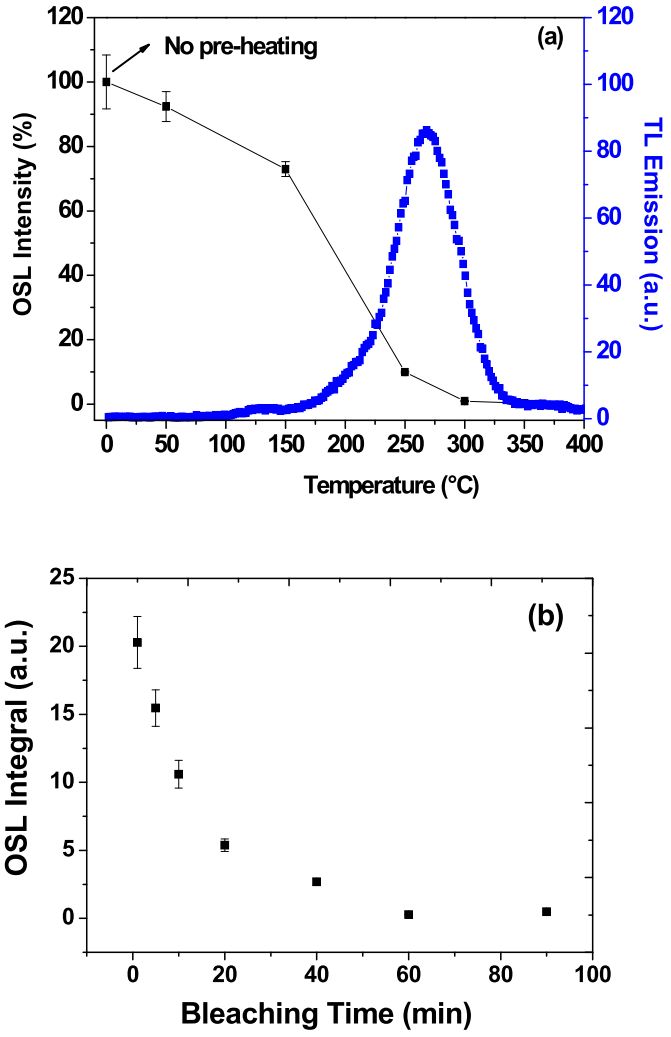

Fig. 5. (a) Step-annealing test, where the OSL signal of MgB_4O_7:Ce,Li is shown as a function of pre-heat temperatures; the typical TL glow curve of the material is also depicted. (b) OSL signal as a function of different exposition times to blue LEDs; in order to restore the initial conditions of the OSLD, the OSL integral was subtracted by the background signal of the pellets. (For interpretation of the references to colour in this figure legend, the reader is referred to the Web version of this article.)

basic requirement for a luminescent material to be applied as 2D detector is that it should have a very low luminescence lifetime decay to avoid the image blurring effect (Ahmed et al., 2016a, 2016b). Recently, the Al_2O_3:C has been suggested as a 2D detector, but the lifetime emission of its main luminescent center (F-center) is 35 ms, and during the film scanning the luminescence of each pixel will contaminate the following one and so on, causing a very strong blurring in the final image, which requires a series of corrections, making the practice cumbersome (Ahmed et al., 2014, 2016b).

3.4. Basic OSL properties

At Fig. 5(a) are shown the results of the step annealing test, where it is possible to correlate the TL and OSL dynamics in the host matrix (Yukihara and McKeever, 2011; Yukihara et al., 2017). The graph shows that a pre-heating of the samples until 150 °C induces a decrease of 25% in the OSL signal, suggesting the presence of shallow traps in the band gap MgB_4O_7. In fact, the TL glow curve of MgB_4O_7:Ce,Li depicted at Fig. 5(a) is composed by an emission in the low temperature range (100–150 °C), which explains the decrease of the OSL signal with the pre-heating until 150 °C.

Pre-heating the samples, from 150 °C up to 350 °C, deplete all the OSL signal of MgB_4O_7:Ce,Li, meaning that the main traps responsible for the OSL signal are located at deep levels in the band gap, which are very stable and so the OSL signal has very low fading (Souza et al., 2017). Previous works showed that MgB_4O_7:Ce,Li have a very low fading in the first days (< 5%), due to the presence of shallow and unstable traps in the band gap, and afterwards no significant fading was observed, which means that most part of the traps responsible for the OSL signal in the host is composed by deep traps (Souza et al., 2017).

From this results, it can be also concluded that the OSL signal of the MgB_4O_7:Ce,Li can be successfully depleted upon heating the samples until 350 °C, but thermal treatment to re-use of TLD/OSLD can change the sensitivity of the detector, which is one of the main drawbacks of the TL technique (Yukihara and McKeever, 2011). So, the best condition to re-use the pellets upon optical bleaching was evaluated. The results in Fig. 5(b) show that exposing the samples to blue LEDs for 60 min is effective to deplete the traps and reestablishes the initial conditions for reuse of the pellets.

The OSL decay curve of MgB_4O_7:Ce,Li, which is shown at Fig. 6(a), was well fitted (χ^2 = 0,996) by a double exponential decay as described in Equation (2):

$$I = I_0 + A_1 e^{\left(\frac{-x}{\tau_1}\right)} + A_2 e^{\left(\frac{-x}{\tau_2}\right)} \quad (2)$$

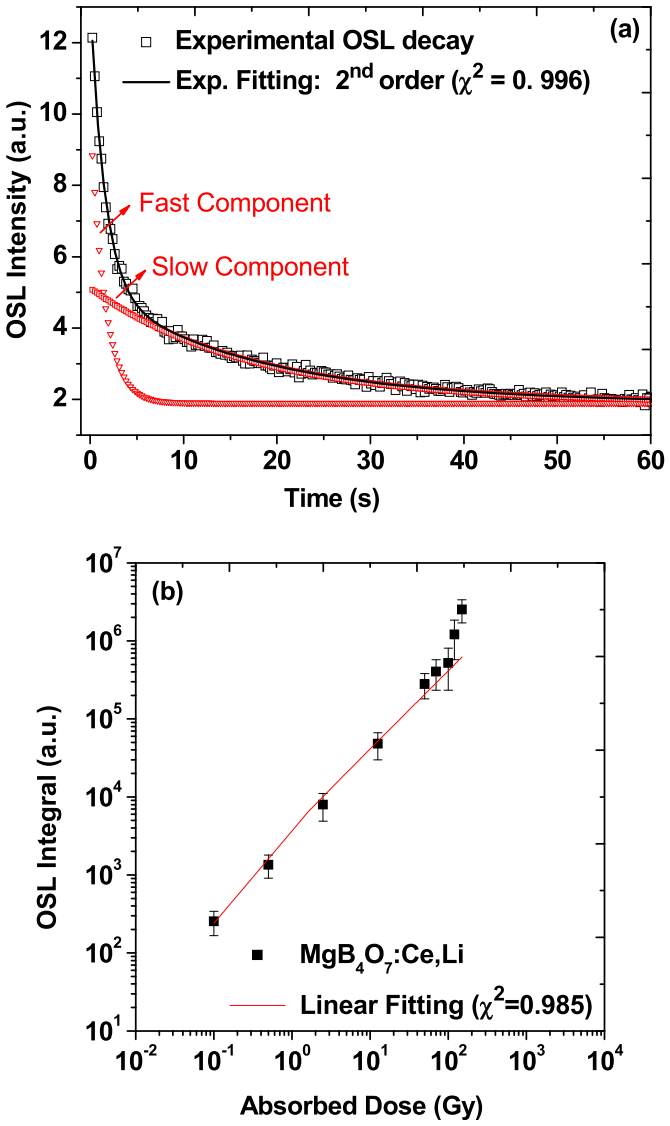

Fig. 6. (a) 2nd order exponential fitting of MgB_4O_7:Ce,Li OSL decay and its main components (fast and slow). In this case, the background signal was not subtracted from the OSL decay curve (b) Dose-response curve of MgB_4O_7:Ce,Li based on total area under the OSL curve (absorbed dose of 0.1 Gy–150 Gy of $^{90}Sr/^{90}Y$).

where I is the luminescent intensity as a function of time, I_0 is the background intensity, A_1 and A_2 are constants and τ_1 = (1.51 ± 0.03)s and τ_2 = (17.4 ± 0.5)s are the lifetimes of the fast and slow components of the OSL decay curve. It is important to keep in mind that in the equation, τ_1 and τ_2 are the time intervals required to the charges to recombine and produce the OSL phenomena, not the intracenter fluorescence lifetime of Ce described at Section 3.3. The fast component is assigned to the direct recombination of electrons and holes, and the slow one is due to the re-trapping of the charges, during several seconds, before being recombined with holes (Souza et al., 2017). Finally, the dose response curve of the pellets is shown in Fig. 6(b), with linear behavior until 100 Gy, and above this value a supralinearity can be observed, which is a very common behavior when the traps are approaching the saturation (Souza et al., 2017; Yukihara et al., 2017). The abrupt increase in the OSL signal, above 100 Gy, maybe related to saturation in the traps, and above this dose the samples cannot be used because the signal is not reliable, and the relative standard errors are too high, approaching 40%. The MDD obtained for the MgB_4O_7:Ce,Li pellets was (1.00 ± 0.10) mGy.

4. Conclusions

The luminescent and basic OSL properties of MgB_4O_7:Ce,Li produced by solid state synthesis were investigated in this work. Initially, the XRD results showed that the MgB_4O_7 can be successfully produced through the solid-state synthesis. The TL and PL emission spectra indicated that the emissions in the UV-VIS region, with peaks located between 350 nm and 400 nm, are due to Ce^{3+} transitions. The lifetimes of these emissions are around 0.003 ms (3 μs), which is 10000 times less than the lifetime of the commercial Al_2O_3:C (F centers), indicating strongly that the MgB_4O_7:Ce,Li is applicable for scanning in 2D dosimetry. The optimal co-dopant concentration for the matrix is 0.5% of Li, which also enlights the effectiveness of the synthesis in incorporating the dopants and co-dopants in the crystalline host. From the step annealing experiment, it was observed that the OSL signal is assigned to shallow (< 150 °C) and deep traps (> 150 °C), and that MgB_4O_7:Ce,Li can be reused successfully (bleaching process) upon exposing it to blue LEDs for 60 min. The dose-response curve is linear up to 100 Gy, and then a supralinear behavior is observed. The MDD obtained for the pellets was around 1 mGy, which increases the range of applications of this material in medical dosimetry. The results demonstrate that MgB_4O_7:Ce,Li fulfills many criteria for an OSL dosimeter be considered efficient, such as: emission in the UV-Vis range, fast lifetime from the main emission centers, low MDD, broad range of linearity in the dose response curve. Moreover, it is to be expected that the 3 mm diameter pellets studied in this work may be easily inserted into body cavities under complex geometries for *in vivo* dosimetry.

Acknowledgments

The authors gratefully acknowledge the support received from the Brazilian agencies CNPq (152654/2016-0, fellowship of L. F. Souza), CNPq (3013352016-8; 427010/2016-0), FAPESP (Process number 2014/12732-9, fellowship of P. L. Antonio), CAPES (88881.119743/2016-01).

References

Ahmed, M.F., Eller, S.A., Schnell, E., Ahmad, S., Akselrod, M.S., Hanson, O.D., Yukihara, E.G., 2014. Development of a 2D dosimetry system based on the optically stimulated luminescence of Al_2O_3. Radiat. Meas. 71, 187–192.
Ahmed, M.F., Schnell, E., Ahmad, S., Yukihara, E.G., 2016a. Image reconstruction algorithm for optically stimulated luminescence 2D dosimetry using laser-scanned Al_2O_3:C and Al_2O_3:C,Mg films. Phys. Med. Biol. 61, 7484–7506.
Ahmed, M.F., Shrestha, N., Schnell, E., Ahmad, S., Akselrod, M.S., Yukihara, E.G., 2016b. Characterization of Al_2O_3 optically stimulated luminescence films for 2D dosimetry using a 6 MV photon beam. Phys. Med. Biol. 61, 7551–7570.
Akselrod, M.S., Botter-Jensen, L., McKeever, S.W.S., 2007. Optically stimulated luminescence and its use in medical dosimetry. Radiat. Meas. 41, S78–S99.
Azorin, J., 2014. Preparation methods of thermoluminescent materials for dosimetric applications: An overview. Appl. Radiat. Isot. 83, 187–191.
Bos, A.J., Dorenbos, P., Bessiere, A., Lecointre, A., Bedu, M., Bettineli, M., Piccineli, F., 2011. Study of TL glow curves of YPO_4 double doped with lanthanide ions. Radiat. Meas. 56, 1410–1416.
Dorenbos, P., 2000. The 5d level positions of the trivalent lanthanides in inorganic compounds. J. Lumin. 91, 155–176.
Doull, B.A., Oliveira, L.C., Wang, D.Y., Milliken, E.D., Yukihara, E.G., 2014. Thermoluminescent properties of lithium borate, magnesium borate and calcium sulfate developed for temperature sensing. J. Lumin. 146, 408–417.
Jahn, A., Sommer, M., Henniger, J., 2010. 2D-OSL-dosimetry with beryllium oxide. Radiat. Meas. 45, 674–676.
Kindrat, I.I., Padlyak, B.V., Mahlik, S., Kukliński, B., Kulyk, Y.O., 2016. Spectroscopic properties of the Ce-doped borate glasses. Opt. Mater. 59, 20–27.
Kumar, V., Pitale, S.S., Mishra, V., Nagpure, I.M., Biggs, M.M., Ntwaeaborwa, O.M., C Swart, H., 2010. Luminescence investigations of Ce^{3+} doped CaS nanophosphors. J. Alloy. Comp. 492, 1–2.
McKeever, S.W.S., 2001. Optically stimulated luminescence dosimetry. Nucl. Instrum. Methods B 184, 29–54.
Oliveira, T.M., Lima, A.F., Brik, M.G., Souza, S.O., Lalic, M.V., 2016a. Electronic structure and optical properties of magnesium tetraborate: An ab initio study. Comput. Mater. Sci. 124, 1–7.
Oliveira, L.C., Yukihara, E.G., Baffa, O., 2016b. MgO:Li,Ce,Sm as a high-sensitivity material for Optically Stimulated Luminescence dosimetry. Sci. Rep. 6, 24348.
Orante-Barron, V.R., Oliveira, L.C., Kelly, J.B., Milliken, E.D., Denis, G., Jacobsohn, L.G.,

Yukihara, E.G., 2011. Luminescence properties of MgO produced by solution combustion synthesis and doped with lanthanides and Li. J. Lumin. 131, 1058–1065.
Poma, P.Y., Santos, W.Q., Sales, T.O., Gouveia-Neto, A.S., Jacinto, C., 2017. Tunable light emission mediated by energy transfer in Tm3+/Dy3+ co-doped LaF3 nanocrystals under UV excitation. J. Lumin. 188, 18–23.
Prokic, M., 1980. Development of highly sensitive $CaSO_4$:D_y/Tm and MgB_4O_7:Dy/Tm sintered thermoluminescent dosimeters. Nucl. Instrum. Methods 175, 83–85.
Prokic, M., 1986. Magnesium borate in TL dosimetry. Radiat. Protect. Dosim. 17, 393–396.
Prokic, M., 1993. MgB_4O_7:Mn as a new TL dosemeter. Radiat. Protect. Dosim. 47, 191–193.
Prokic, M., 2000. Effect of lithium co-dopant on the thermoluminescence response of some phosphors. Appl. Radiat. Isot. 52, 97–103.
Prokic, M., 2007. Individual monitoring based on magnesium borate. Radiat. Protect. Dosim. 125, 247–250.
Prokic, M., Botter, J., 1993. Comparison of main thermoluminescent properties of some TL dosimeters. Radiat. Protect. Dosim. 47, 185–199.
Rao, M.R., Rao, B.S., Rao, N.P., Omaiah, K., Murthy, K.V.R., 2009. Thermoluminescence characteristics of MgB_4O_7, MgB_4O_7:Mn and MgB_4O_7:Cu phosphors. Indian J. Pure Appl. Phys. 47, 456–458.
Sommer, M., Jahn, A., Henniger, J., 2008. Beryllium oxide as optically stimulated luminescence dosimeter. Radiat. Meas. 43, 353–356.
Souza, L.F., Vidal, R.M., Souza, S.O., Souza, D.N., 2014. Thermoluminescent dosimetric comparison for two different MgB_4O_7:Dy production routes. Radiat. Phys. Chem. 104, 100–103.
Souza, L.F., Antonio, P.L., Caldas, L.V.E., Souza, D.N., 2015. Neodymium as a magnesium tetraborate matrix dopant and its applicability in dosimetry and as a temperature sensor. Nucl. Instrum. Methods A. 784, 9–13.
Souza, L.F., Silva, A.M.B., Antonio, P.L., Caldas, L.V.E., Souza, S.O., d'Errico, F., Souza, D.N., 2017. Dosimetric properties of MgB_4O_7:Dy,Li and MgB_4O_7:Ce,Li for optically stimulated luminescence applications. Radiat. Meas. 106, 196–199.
Subanakov, A.K., Bazarova, Z.H.G., Nepomnyshchikh, A.I., Perevalov, A.V., Bazarov, B.G., 2014. Synthesis and characterization of dysprosium doped magnesium tetraborate. Inorg. Mater. 50, 485–488.
Twardak, A., Bilski, P., Zorenko, Y., Gorbenko, V., Sidletskiy, O., 2014. OSL dosimetric properties of cerium doped lutetium orthosilicates. Radiat. Meas. 71, 139–142.
Yukihara, E.G., McKeever, S.W.S., 2011. Optically Stimulated Luminescence: Fundamentals and Applications. John Wiley & Sons Ltd, United Kingdom.
Yukihara, E.G., Milliken, E.D., Oliveira, L.C., Orante-Barro, V.R., Jacobsohn, L.G., Blair, M.W., 2013. Systematic development of new thermoluminescence and optically stimulated luminescence materials. J. Lumin. 133, 203–210.
Yukihara, E., Milliken, E., Doull, B., 2014. Thermally stimulated and recombination processes in MgB_4O_7 investigated by lanthanide doping. J. Lumin. 154, 251–259.
Yukihara, E.G., Doull, B.A., Gustafson, T.L., Oliveira, C., Kurt, K., Milliken, E.D., 2017. Optically Stimulated Luminescence of MgB_4O_7:Ce,Li for gamma and neutron dosimetry. J. Lumin. 183, 525–532.